

## Deadline for Nominations: 15 September 1977

### AAAS–Newcomb Cleveland Prize: Contest Year Is Nearly Over

The deadline for nominations of papers for the AAAS–Newcomb Cleveland Prize is fast approaching. Readers are invited to nominate papers published in the Reports section of *Science* from 3 September 1976 to 26 August 1977. The prize of \$5000 and a bronze medal is now given annually to the author of an outstanding paper that is a first-time publication of the author's own research.

Nominations must be typed and the following information provided: the title of the paper, issue in which it was published, author's name, and a brief statement of justification for nomination. Nominations should be submitted to AAAS–Newcomb Cleveland

Prize, AAAS, 1515 Massachusetts Avenue, NW, Washington, D.C. 20005. Final selection will rest with a panel of distinguished scientists appointed by the Board of Directors.

The award will be presented at a session of the annual meeting at which the winner will be invited to present a scientific paper reviewing the field related to the prizewinning research. The review paper will subsequently be published in *Science*. In cases of multiple authorship, the prize will be divided equally between or among the authors; the senior author will be invited to speak at the annual meeting.

## Reports

### Detection of Lyman $\alpha$ Emission from the Saturnian Disk and from the Ring System

*Abstract. A rocket-borne spectrograph detected H I Lyman  $\alpha$  emission from the disk of Saturn and from the vicinity of the planet. The signal is consistent with an emission brightness of 700 rayleighs for the disk and 200 rayleighs for the vicinity of Saturn. The emission from the vicinity of the planet may be due to a hydrogen atmosphere associated with the saturnian ring system.*

Radiation of the type H I Lyman  $\alpha$  (1216 Å) has been detected from only one of the outer planets, namely Jupiter, with a reported brightness on the order of 2 kilorayleighs ( $I$ ) [ $1 \text{ rayleigh (R)} = 10^6/4\pi \text{ photon cm}^{-2} \text{ sec}^{-1} \text{ ster}^{-1}$ ]. Resonance scattering of solar Ly  $\alpha$  and charged particle excitation in the outer atmosphere of Jupiter are thought to be the principal mechanisms for this spectral emission. It is reasonable to assume that mechanisms that give rise to H I emission in the jovian atmosphere may also be operating in the atmosphere of Saturn. This emission provides information on both the excitation mechanisms and the constituents of the upper atmosphere. In addition, if there is an atmosphere caused by outgassing from ring material, Ly  $\alpha$  emission from the vicinity of Saturn is an indicator. Finally, the values of the Ly  $\alpha$  emissions are also of use for the Mariner mission (Voyager) to Jupiter and Saturn, to be launched late in the summer of 1977.

Since the solar radiation incident at Saturn is smaller by a factor of 3.5 than

that at Jupiter, one can expect a saturnian Ly  $\alpha$  disk brightness of several hundred rayleighs or less. This lower brightness in addition to the fact that the saturnian disk subtends only 1/6 the solid angle of Jupiter (both planets at opposition) results in an expected saturnian Ly  $\alpha$  flux at Earth that is more than 20 times weaker than the Ly  $\alpha$  radiation coming from Jupiter. In addition, a strong Ly  $\alpha$  background signal (typically 1 to 3 kR) due to terrestrial airglow makes detection of saturnian Ly  $\alpha$  radiation even more difficult.

A statistically significant detection of Ly  $\alpha$  emission from Saturn was obtained, for the first time to our knowledge, by a sounding rocket launched from the White Sands Missile Range, New Mexico, in March 1975. The rocket carried a 36-cm telescope and a sensitive spectrograph with a microchannel plate detector and obtained far-ultraviolet spectra (1160 to 1750 Å) of Saturn and two cool stars ( $\alpha$  Aur and  $\alpha$  Boo). The fine tracking capability of the telescope made it possible to point to 1 arc sec and

permitted the use of very small spectrograph entrance apertures, thus reducing the background signal due to Ly  $\alpha$  radiation from terrestrial airglow. A microchannel plate detection system made it possible to observe all spectral elements simultaneously and avoided the need for spectral scanning. The improvement in sensitivity of this instrument as compared to the single-slit scanning spectrometers flown on earlier missions by this laboratory was greater than a factor of 20 at 1216 Å (2).

The spectrograph, a dual-channel Czerny Turner with a LiF prism (2), recorded the spectrum of the target with one channel while the other channel monitored the spectrum of the airglow background over the same wavelength range from an area in the sky with a diameter of 58 arc sec, 400 arc sec away from the target. Two entrance apertures (diameters, 26 and 53 arc sec) were selected in flight for the target channel; their alternate use during the Saturn observation (5 seconds each, for a total observing time of 110 seconds) made it possible to distinguish between the spectrum emitted by the saturnian disk and that emitted by the total disk-ring system.

At the time of observation, Saturn's disk had an angular extent of 17 by 19 arc sec; the outer edge of ring A had an extent of 43 by 19 arc sec. The ring inclination and the phase angle were 26° and 6°, respectively, close to their maximum values. The geometry of the various entrance apertures with respect to the saturnian system at the time of observation is shown in Fig. 1.

From the data of Fig. 2, we derive a Ly  $\alpha$  brightness of 700 R  $\pm$  50 percent for the saturnian disk and 200 R  $\pm$  50 percent for the vicinity of the disk; we did this by assuming that the source for

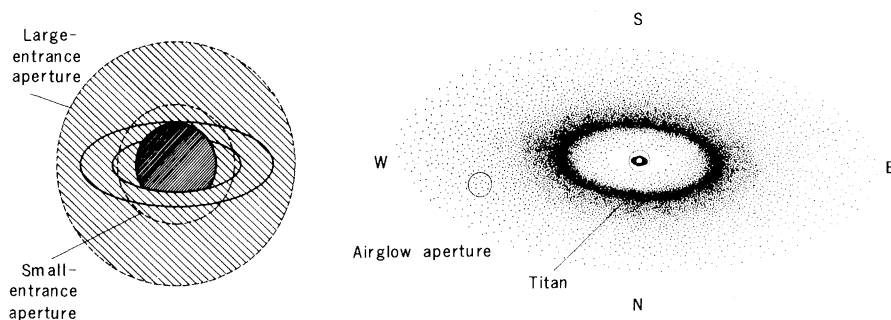


Fig. 1. Geometry of the various entrance apertures with respect to the saturnian system at the time of observation. The dotted area around the orbit of Titan depicts the toroidal hydrogen cloud proposed by McDonough and Brice (3). The expected variation of the H I Ly  $\alpha$  brightness is indicated by the density of the dots. The diagram on the left shows the central portion in greater detail and also indicates with different shading the two Ly  $\alpha$  source regions discussed in the text.

the 700-R signal was identical with the geometric disk of Saturn whereas the 200-R signal came from an area outside and immediately adjacent to the disk, filling the remaining area of the large-entrance aperture (see Fig. 1). In this case, a uniform brightness level has been assumed for each of the two source regions. Since spatial variations are expected, the quoted values should be treated only as averages. The exact values obtained depend on the model assumed for the spatial distribution of the radiation. As an example, if the Ly  $\alpha$  signal from outside the disk were to originate solely in rings A and B, the resulting ring brightness would be  $\sim 1000$  R and the disk brightness would be undetermined ( $200 \pm 400$  R). The other extreme, a zero Ly  $\alpha$  brightness contribution from the region surrounding the planet, is not compatible with our data, since the change in signal between large and small aperture strongly indicates that the emission came from the vicinity as well as the disk of the planet.

The uncertainties in the Ly  $\alpha$  brightnesses quoted above are not a measure of the statistical significance of the detection of Ly  $\alpha$  emission. The small-aperture saturnian Ly  $\alpha$  signal exceeded the background airglow Ly  $\alpha$  (1.3 kR at the time of observation) with a statistical significance of  $3\sigma$  (99.7 percent), where  $\sigma$  is the standard deviation, the large-aperture signal with a significance of  $5\sigma$ . These standard deviations are based on Poisson statistics and the observed numbers of photon events. Laboratory tests showed that, to a very high precision, the detector exhibited Poisson statistics, indicating that the statistical uncertainty estimates are reliable (2). A 20 percent calibration uncertainty and the combination of the large- and small-aperture data used to derive Ly  $\alpha$  brightnesses for the disk and rings gave the 50 percent uncertainty of the Ly  $\alpha$  brightness values

quoted above. Other errors, such as drifts of the detector or of optical components of the two spectrograph channels, were possible but not very likely. In both airglow and target channels the same spectrograph optics and adjacent areas of the same microchannel plates were used. In addition, there were no drifts in the measured values during the observation period (Fig. 2), and during transition maneuvers (*T* in Fig. 2) the airglow-corrected Ly  $\alpha$  values went to zero.

The observations of Saturn were made above an altitude of 160 km; most of the data were acquired near the rocket apogee of 211 km. Because of a Doppler shift of  $0.11 \text{ \AA}$ , less than 5 percent absorption by terrestrial H was expected and no correction was made. A time-dependent correction for absorption by the outgassing of H<sub>2</sub>O vapor from the rocket was made for both channels of the

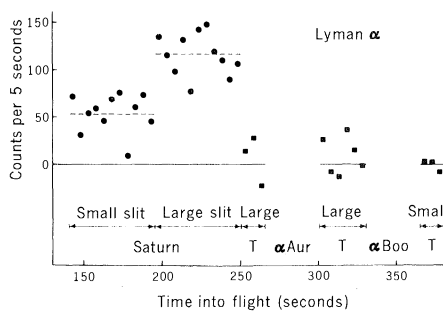


Fig. 2. The Ly  $\alpha$  signal from the saturnian system obtained during flight. Circles are Saturn data for both the small and the large entrance aperture; squares are data obtained during the transition maneuvers (*T*) of the rocket between targets when essentially only sky background was observed. The data are corrected for airglow, H<sub>2</sub>O vapor absorption, and dark count. Each data point represents the integrated counts over a 5-second period; the large- and small-aperture observations on Saturn, which alternated during the flight, have been grouped together for clarity. The Ly  $\alpha$  data during the  $\alpha$  Aur and  $\alpha$  Boo observation are off scale and have been omitted.

spectrograph. However, it was quite small, 30 percent at the beginning, decreasing exponentially with a time constant of 30 seconds. An in-flight sensitivity comparison at  $1216 \text{ \AA}$  was obtained by a simultaneous independent observation of  $\alpha$  Boo made by the Orbiting Astronomical Observatory Copernicus satellite. Good agreement between the Ly  $\alpha$  fluxes, well within the uncertainty limits of the two instruments, was obtained (2).

According to a recent model (3), the saturnian system is surrounded by a toroidal cloud of hydrogen centered around the orbit of Titan and extending to a distance of as much as 60 saturnian radii. The Ly  $\alpha$  brightness in the outermost parts of the cloud where the airglow slit was located (see Fig. 1) is expected to be quite small, probably not more than a few rayleighs; it has therefore been neglected. A nonvanishing contribution of the hydrogen torus to the airglow measurement would only have the effect of increasing the brightness values for the saturnian disk and ring system quoted above.

The 700-R Ly  $\alpha$  brightness of the saturnian disk scales quite well (geometric scaling factor 3.5) with the 2-kR jovian Ly  $\alpha$  emission reported (1). This value—which is model-dependent—might indicate similar excitation mechanisms for Ly  $\alpha$  in the upper atmospheres of both Jupiter and Saturn (4). The 200-R signal from the ring system is somewhat puzzling. According to theoretical estimates (5), the rings are expected to have an atmosphere of H, H<sub>2</sub>, and H<sub>2</sub>O which is created by local heating and evaporation of the H<sub>2</sub>O ice cover of the ring particles. The H<sub>2</sub>O can in turn be photodissociated and thus become an important source for H. However, the production rates for processes such as meteoroid bombardment, solar wind bombardment, interstellar wind bombardment, and ice sublimation are such that the number density for H in the ring vicinity would only be 1 to  $10 \text{ cm}^{-3}$ , thus giving rise to a Ly  $\alpha$  luminosity of the rings that is on the order of only 10 R. Possible reasons for this discrepancy could be low estimates in the production rates or contributions from processes not considered so far. For example, the H<sub>2</sub>O production by ice sublimation is very uncertain since it depends critically upon the temperature of the rings (6) and estimates of the sublimation rate.

H. WEISER  
R. C. VITZ  
H. W. MOOS

Department of Physics,  
Johns Hopkins University,  
Baltimore, Maryland 21218

## References and Notes

1. G. J. Giles, H. W. Moos, W. R. McKinney, *J. Geophys. Res.* **81**, 5797 (1976).
2. H. Weiser, R. C. Vitz, H. W. Moos, A. Weinstein, *Appl. Opt.* **15**, 3123 (1976).
3. T. R. McDonough and N. M. Brice, *Icarus* **20**, 136 (1973).
4. D. F. Strobel, *Rev. Geophys. Space Phys.* **13**, 372 (1975).
5. J. E. Blamont, in *Proceedings of the Saturn Ring Workshop*, F. D. Palluconi and G. H. Pettengill, Eds. (Science Publication 343, National Aeronautics and Space Administration, Washington, D.C., 1973), p. 125; M. Dennefeld, *Int. Astron. Union Symp.* **65**, (1974), p. 471.
6. J. B. Pollack, *Space Sci. Rev.* **18**, 3 (1975).
7. This research was supported under NASA grant NGR 21-001-001. The rocket was prepared and launched by the Sounding Rocket Division of Goddard Space Flight Center, Greenbelt, Maryland.

7 February 1977; revised 6 May 1977

## Multistranded Helix in Xanthan Polysaccharide

**Abstract.** *The extracellular polysaccharide xanthan is shown by electron microscopy to be an unbranched, probably double-stranded fiber 4 nanometers wide and 2 to 10 micrometers long when native. Denaturation yields a single strand only 2 nanometers wide and 0.3 to 1.8 micrometers long. Renatured xanthan shows short unraveled regions with two or three strands arranged in a right-handed twist.*

The extracellular polysaccharide xanthan produced by the microorganism *Xanthomonas campestris* finds extensive use as a viscosity-enhancing agent because of its high-specific viscosity and striking pseudoplasticity (1). It is already widely used in foods; in addition, there is a large potential application in chemically enhanced oil recovery (2). The primary structure of the polymer was recently shown to consist of a main chain made up of  $\beta$ -(1 $\rightarrow$ 4)-linked D-glucose, as in cellulose, but with a 3-sugar side chain attached at C(3) to alternate glucose residues of the main chain (3). The side chain is  $\beta$ -D-mannose-(1 $\rightarrow$ 4)- $\beta$ -D-glucuronic acid-(1 $\rightarrow$ 2)- $\alpha$ -D-mannose-6-O-acetyl. About one-third of the terminal mannose residues bear a pyruvic acid acetal. Because of the glucuronic acid and pyruvate groups, xanthan exhibits many typical polyelectrolyte properties.

The secondary and tertiary structures of xanthan are still largely unknown. X-ray scattering from xanthan fibers of poor crystallinity shows a helix with fivefold symmetry and pitch 4.70 nm (4, 5). The pattern has been tentatively interpreted in terms of a single-stranded structure, but a double-helical model has not been ruled out (5). Previous solution studies give strong hints of an ordered native conformation. For example, when dissolved in water of low ionic strength, xanthan exhibits a thermally induced conformational transition between a native, probably rodlike structure and a more flexible denatured conformation. This transition, which was first observed by Jeanes and her co-workers (6), has until now been characterized only by viscosity measurements (6-9), optical rotation or circular dichroism (7-10), and nuclear magnetic resonance (10). To elucidate this structural change more fully, we have obtained electron micrographs and molecular filtration chromatograms

of native, denatured, and renatured xanthan.

Purified native xanthan was prepared from dried commercial powder or from undried culture broths by methods previously described (11). Similar results were obtained whether or not the sample had been dried or precipitated at any time in its history. Denatured xanthan was prepared by heating a dilute solution of the native polymer (in deionized water at pH 6 to 7) to 95°C for 15 minutes, then quenching the solution in ice water. The denatured polymer thus obtained exhibited at 5°C optical rotation characteristics of the denatured state at high temperatures (9). The optical rotation of such a denatured polysaccharide solu-

tion in deionized water remained unchanged for many days at 5°C. However, if a small amount of NaCl (0.01 to 0.04M) was added to the denatured sample, the optical rotation immediately returned to that of the native form (9). We term this a renatured sample. Strikingly similar salt-dependent thermal denaturation and renaturation occur in triple-standard collagen and double-stranded polynucleotides (12). In preparing renatured xanthan samples for electron microscopy, the NaCl was replaced through dialysis by 0.01M ammonium acetate, pH 7.

Electron micrographs of xanthan were obtained by a novel but simple technique, which involves the use of what we call a reactive carbon substrate. Normally, when one prepares carbon substrates the carbon is evaporated at the lowest convenient pressure, usually about  $10^{-6}$  torr. For our reactive films, however, the carbon was evaporated with  $10^{-3}$  to  $10^{-4}$  torr of air remaining; this is the point at which the carbon begins to spark instead of evaporating smoothly. The resulting carbon films have carboxyl, phenol, keto, and quinone groups incorporated in the film's surface. These groups act as reactive sites for the deposition of the polysaccharide.

A microdrop of a solution with a xanthan concentration of 6 parts per million was placed in the center of a standard electron microscope grid covered with the carbon film and allowed to dry in the air of a dust-free, laminar-flow hood. Ap-

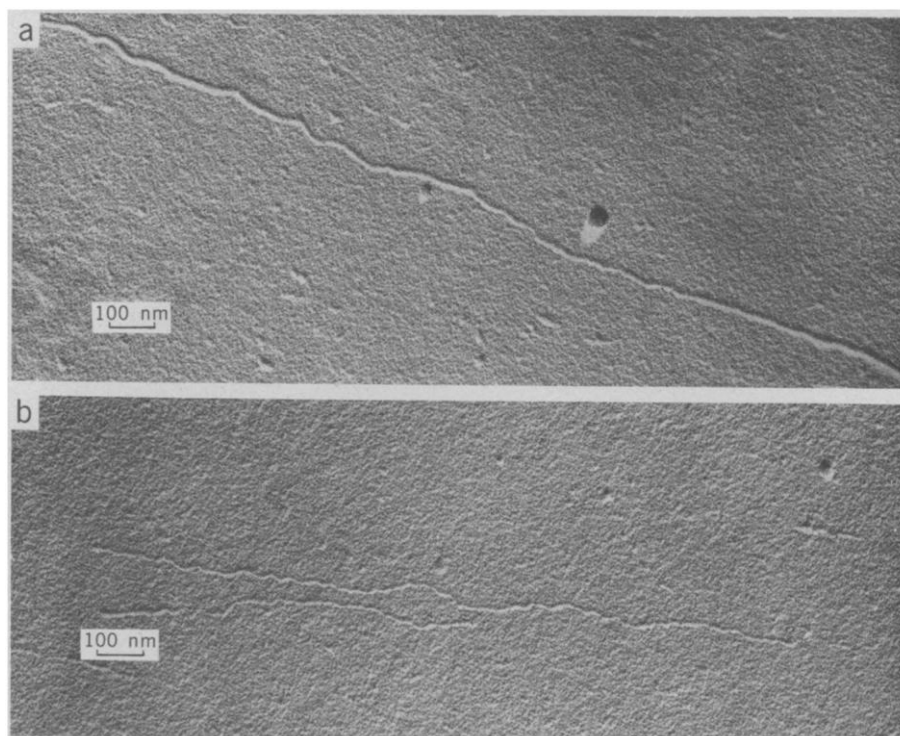


Fig. 1. (a) Electron micrograph of a portion of a native xanthan molecule. At this magnification this molecule would extend over six frames of this size. (b) Denatured xanthan molecules.